CHARACTERIZATION OF OCTAMETHYLSILSESQUIOXANE $(CH_3)_8Si_8O_{12}$ FILLERS IN POLYPROPYLENE MATRIX

S. Virtanen[1ab], T. Kortelainen[2], Susanna Ahonen[1ab], V. Koivu[3], M. Lahtinen[1b], E. Arola[2,4], M. Karttunen[5], S. Kortet[5], K. Kannus[4] and M. Pettersson[1ab]

[1]*Nanoscience Center[a], Department of Chemistry[b], P.O.Box 35, FI-40014 University of Jyväskylä, Finland*

[2]*Department of Physics, Tampere University of Technology, P.O. Box 692, 33101, Tampere,*

[3]*Department of Physics, P. O. Box 35, FI-40014 University of Jyväskylä, Finland*

Finland

[4]*Department of Electrical Energy Engineering, Tampere University of Technology, P.O.Box 692, 33101 Tampere, Finland*

[5]*Technical Research Centre of Finland, P.O.Box 1607, 33101 Tampere, Finland*

Abstract

The results of Raman microspectroscopy measurements of octamethylsilsesquioxane (om-POSS) (3-wt %) in polypropylene (PP) are presented and compared with theoretical spectra calculated by ab initio density functional theory (DFT) based methods. The internal structure of this dielectric composite at the micrometer level was obtained by Computerized X-ray micro-tomography (CXμT) which reveals how micron-scale filler particles are distributed in the matrix media. The X–ray powder diffraction (XPD) was used to determine the om-POSS inner crystallite size that is in a nanometer range. Transmission electron microscopy (TEM) images confirm that the composite contains both nano and micron sized particles. The multiscale analysis indicates that in the composite om-POSS crystalline nanoparticles having a size from tens to hundreds of nanometers tend to agglomerate together with preferred orientation to form elongated micron sized particles. Orientation of crystallites affects the relative intensity of various Raman peaks. Appearance of Raman images thus depends on the choice of the peak used in the analysis.

1. Introduction

POSS-based (polyhedral oligomeric silsesquioxane) materials, including biomaterials, dielectric materials, organic light-emitting diodes, lithography resists, catalysts, membrane fuel cells, and battery membranes have recently been introduced [1]. Advantageous changes in the material properties of nanocomposites are usually connected with the surface properties and interfacial interaction of the filler particles because of the large surface area to volume ratio of the filling material. Hence, properties such as structure and orientation of the filler in the polymer matrix may play a crucial role in understanding this phenomenon. The octamethyl-POSS (om-POSS) filler material has been shown to have ability to substantially increase the breakdown strength of polypropylene (PP) [2]. The results of the relative permittivity, loss factor and volume resistivity measurements indicate that om-POSS additives could improve the dielectric properties of PP.
In this work we present detailed structural analysis of this om-POSS-PP composite material. In particular we explain the variation in the Raman spectrum of om-POSS particles.

2. Methods

2.1. Raman microspectroscopy

For composite analysis a dispersive micro-Raman spectrometer (Bruker Senterra R200-785) equipped with a linearly polarized diode laser (785 nm) in back-scattering geometry was used. The confocal aperture used was 25 μm with 100x objective (NA 0.90). The laser power was kept low to avoid overheating the sample (25 mW). At each point measurement time was 10 s. The area of interest in the sample was scanned with motorized stage of 0.1 μm accuracy in two or three dimensions using 0.5 μm steps.

2.1.1 Theoretical analysis of Raman spectra

In this work angular dependence of the Raman spectrum of the om-POSS crystal is studied theoretically using Raman susceptibility tensor calculated with the state-of-the-art code Abinit [3, 4] and rotating the tensor $\mathbf{R}^m$ of the formula

$$I \propto |e_s \mathbf{R}^m e_i|^2$$

where e_s and e_i are the unit polarization vectors of the scattered and incident laser fields.
In density functional theory calculation, Perdew-Wang 92 functional, Monkhorst Pack [5] k-point grid and energy cut off 4×4×4 / 500 eV with Troullier Martins pseudopotentials have been used. The details of the calculation have been described elsewhere [6].

2.2. X–ray powder diffraction (XPD)

The X–ray powder diffraction data was measured with PANalytical X´Pert PRO diffractometer in Bragg–Brentano geometry using two different beam setups. For om-POSS powder, Johansson monochromator was used to produce pure Cu $K_{\alpha 1}$ radiation (1.5406 Å; 45kV, 30mA), and composite sample only β-filter was used to produce mixed Cu K_{α} radiation (1.541874 Å; 45kV, 30mA). The data was collected in continuous step-scanning mode by X´Celerator detector on 2θ range of 4-75° with a step size of 0.0167°, and using sample dependently counting times of 20 or 35 sec per step. Hand-ground powder sample was adhered on a silicon-made zero–background holder with petrolatum jelly, whereas composite sample was placed to a solid-sample bracket. The qualitative search-match routine implemented in HighScorePlus was used for identification of samples with ICDD powder diffraction PDF-2 database (release 2007) [7].

2.3. Computerized X-ray micro-tomography (CXµT)

The composite sample was cut with razor blade to (1.760x0.813x0.339) mm size. The tomographic images of the sample were obtained using SkyScan 1172 -table-top tomographic scanner. 3D image of the sample is calculated from the transmission or reflection data collected by illuminating the object from many different directions. The scanner uses continuous incoherent X-ray beam to produce 2D shadowgraphs from multiple angles. Reconstruction of the shadowgraphs produces cross-sectional images of the absorption coefficients of the X-ray beam. 3D picture of the sample consists of hundreds or thousands of cross-sectional images. Tomographic image had in this case resolution of 0.9 µm. Tomographic imaging noise was removed with variance weighted mean filter before tresholding image to binary geometry, particles and bulk material, for the purpose of 3D particle analysis. Particle volume distribution was determined by an algorithm that analyses the 3D shape of the particles and their volume from binarized image.

2.4. Transmission electron microscopy (TEM)

The nanoscale dispersion of om-POSS in the PP matrix was investigated with TEM. Ultrathin sections of the sample were obtained using a Diatome 45° diamond knife at room temperature using a Leica Reichert Ultracut S ultramicrotome. The 95 nm thick sections were collected on a copper grid and observed with JEOL-JEM-1200EX electron microscope at 60 kV acceleration voltage.

3. Results

3.1. Raman microspectroscopy

The spectra of the PP and om-POSS microparticles were measured (Fig. 1). The spectral range of 120-250 cm^{-1} was selected as an optimal for analysis of om-POSS in composite to avoid overlapping of characteristic Raman peaks of PP. The microparticles in the sample were then scanned and visualized as an intensity contour plot of a selected characteristic Raman peak of om-POSS. The appearance of the intensity contour plot depends on which Raman peak is used in the analysis (Fig. 2). This effect is caused by variation in the relative intensities of different Raman peaks depending on measurement spot (see spectra in Fig. 2). This has to be taken into account when making conclusions about material distribution in the sample.

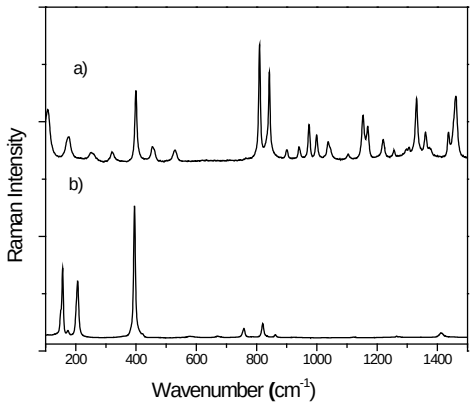

Fig. 1*. Raman spectrum of a) PP b) om-POSS*

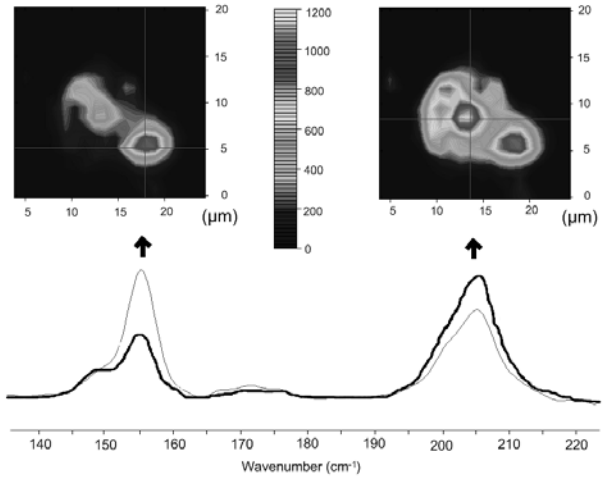

Fig. 2. *Raman intensity contour plots of an om-POSS particle in a composite generated by integrating intensity of the peak at 157 cm^{-1} (left image) and at 206 cm^{-1} (right image). The crosses situated in the intense regions of the contour plots mark the place where the spectra below are collected. The difference in the images reflects the relative difference of the peak intensities in different regions of the agglomerate.*

3.1.1. Theoretical analysis of Raman spectra

Raman spectra of om-POSS crystal were calculated using two different single crystal orientations in linearly polarized electric field. Lorenzian broadened spectra are shown below. (Fig. 3)

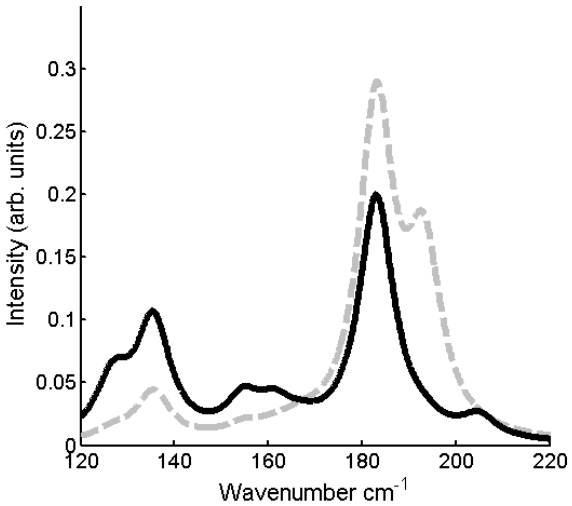

Fig. 3 *Calculated spectra with two different linearly polarized laser and analyzer (parallel) orientations: 60° (gray) and 180° (black) rotation around a trigonal axis of the rhombohedral om-POSS crystal.*

3.2. X–ray powder diffraction (XPD)

The average crystallite sizes of om-POSS were estimated by Scherrer method using the full-width at half-maximum of the most isolated diffraction peak of om-POSS at 10.6° 2θ. The average crystallite sizes were determined to be 170 nm for powder and 40 nm for composite samples.

3.3. Computerized X-ray micro-tomography (CXμT)

The combined volume of the om-POSS particles was determined to be 1.7 % from the total volume of the sample. Taking into account the densities of om-POSS (~1.26 g cm^{-3}) and PP (~0.946 g cm^{-3}) this corresponds to the concentration of 2.3 wt -%. The aspect ratio of the particles was calculated to be 4.6. These elongated particles were evenly distributed in the matrix. (Fig.4) The diameter distribution extends from about 1 μm to 16 μm and the most probable diameter is about 6 μm.

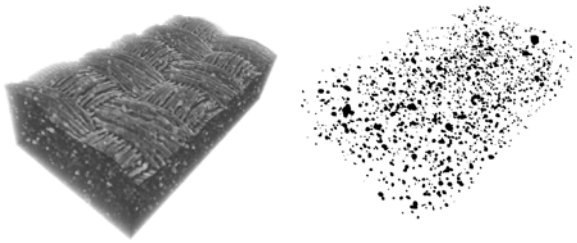

Fig. 4*. CXμT visualization of the total bulk material presented on the left and particle phase on the right. Physical dimensions are (1.760x0.813x0.339) mm.*

3.4. Transmission electron microscopy (TEM)

Micrographs show that most of the om-POSS crystals are agglomerated together in the PP matrix as micro-particles that consist of nanoparticles with various orientations. (Fig. 5)

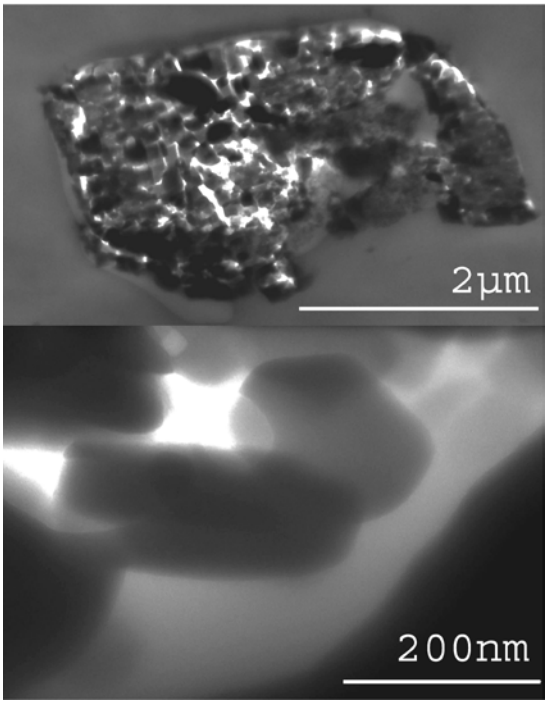

Fig. 5. *TEM images of an om-POSS particle in composite sample.*

4. Discussion

Polycrystalline microparticles give characteristic Raman signal of om-POSS [8, 9] The Raman signal of these particles is not uniform in this material as reported earlier. [2] The optimal spectral range for distinguishing om-POSS from PP is 120-250 cm^{-1}. There are three Raman peaks: 150 cm^{-1}, 157 cm^{-1} and 206 cm^{-1} that can

be assigned to om-POSS. In the spectra the relative intensities of the peaks vary depending on the measurement spot (Fig. 2). The theoretical calculations done by changing the crystal orientation in linearly polarized electric field show qualitatively similar changes in relative peak intensities (Fig.3).

A plausible explanation to this effect is caused by orientation of the crystallites in agglomerates. Tensorial nature of Raman scattering leads to dependence of signal intensity on the relative orientation between the electric field of the incoming electromagnetic field and the molecule. This effect can be easily measured for single crystals [10]. In the present case measurements are performed for polycrystalline agglomerates. Detailed theoretical modelling shows that the orientation effect indeed can explain the variation in the peak intensities observed in this work [6] (see Fig. 3). Thus, we argue that within the confocal volume there must be orientation in the ensemble of individual crystallites. This conclusion points to an interesting possibility of orientational Raman mapping.

A quantitative microstructure analysis done by CXμT reveals that the microparticles are evenly distributed and have elongated shape. Under optical microscope the om-POSS PP-composite appears to be heterogeneous mixture of polycrystalline rod shaped microparticles in semi crystalline polymer matrix. A similar morphology of the same type of composites has been characterized previously using electron microscopy and XPD techniques [11-14].

The XPD analysis gives a crystallite size that is in nanometer scale. TEM images from the composite support this information. Cubic elongated nanocrystals are agglomerated together and form microparticles of specific elongated shape that suggest their packing is not fully random.

5. Conclusion

Composite material consisting of om-POSS and polypropylene was studied by Raman micro-spectroscopy. It was found that the relative intensities of different Raman peaks of om-POSS varied depending on the measurement spot. In order to understand this variation detailed Raman spectroscopic and structural characterization studies complemented by theoretical modelling were performed. Multiscale characterization yielded a detailed picture of the samples consisting of homogeneously distributed micron-sized elongated om-POSS agglomerates. The average size of the crystallites in the agglomerates is on the order of 40 nm. The variation in the Raman spectra of om-POSS can be explained by the orientation of crystallites showing that within the confocal volume there is orientation in the ensemble of crystallites forming large agglomerates. The results are important considering the interpretation of Raman images in composite materials and imply a possibility for orientational imaging.

6. References

[1] Wu, J.; Mather, P.T.; Polymer Reviews 2009, 49, 25-63.

[2] Takala, M.; Karttunen, M.; Salovaara, P.; Kortet, S.; Kannus, K.; Kalliohaka, T. Dielectric Properties of Nanostructured Polypropylene- Polyhedral Oligomeric Silsesquioxane Compounds. IEEE Trans. Dielectr. Electr. Insul. 2008, 15, 40-51.

[3] Gonze, X., Amadon, B., Anglade, P.-M., Beuken, J.-M., Bottin, F., Boulanger, P., Bruneval, F., Caliste, D., Caracas, R., Cote, M., Deuts, T., Hamann, D.R., Hermet, P., Jollet, F., Jomard, G., Leroux, M. Mancini, S. Mazevetch, L. Genovese, Ph. Ghosez, M., Giantomassi, S. Goedecker, Oliveira, M.J.T., Onida, G., Pouillon, Y., Rangel, T., Rignanese, G.M., Sangalli, D., Shaltaf, R., Torrent, M., Verstraete, M.J., Zerah, G., Zwanziger, J.W., Computer Phys.Commun., 2009, 180, 2582.

[4] Gonze, X., Rignanese, G.-M., Verstraete, M.J., Beuken, J.-M., Pouillon, Y., Caracas, R., Jollet, F., Torrent, S., Zerah, G., Mikami, M., Ghosez, Ph., Veithen, M., Raty, J.-Y., Olevano, V., Bruneval, F., Reining, L., Godby, R., Onida, G., Hamann, D.R., Allan. D.C., Zeit. Kristallogr., 2005, 220, 558.

[5] Monkhorst, H.J., Pack, J.D., Special points for Brillouin-zone integrations Physical Review B13, 197, 5188.

[6] Kortelainen, T., et al., manuscript under preparation.

[7] International Centre for Diffraction Data, ICDD-PDF2, Release 2007, 12 Campus Boulevard, Newton Square, Pennsylvania USA.

[8] Handke, B.; Jastrzebski, W.; Mozgawa, W.; Kowalewska, A. Structural Studies of Crystalline Octamethylsilsesquioxane $(CH3)_8Si_8O_{12}$. J. Mol. Struct. 2008, 887, 159-164.

[9] Kolesov, B. A.; Martynova, T. N.; Chupakhina, T. I. Vibration Spectra and Analysis of Normal Vibrations of Octamethylsilsesquioxane. Journal of Structural Chemistry 1989, 29, 888-891.

[10] Mossbrucker, J., Grotjohn, T.A., Determination of local crystal orientation of diamond using polarized Raman spectra, Diamond and Rel. Mat. 1996,5, 1333-1343.

[11] A.; Fina, Tabuani, D.; Frache, A.; Camino, G. Polypropylene-Polyhedral Oligomeric Silsesquioxanes (POSS) Nanocomposites. Polymer 2005, 46, 7855-7866.

[12] Pracella, M.; Chionna, D.; Fina, A.; Tabuani, D.; Frache, A.; Camino, G. Polypropylene-POSS Nanocomposites: Morphology and Crystallization Behaviour. Macromol. Symp. 2006, 234, 59-67.

[13] Chen, J.; Chiou, Y. Crystallization Behavior and Morphological Development of Isotactic Polypropylene Blended with Nanostructured Polyhedral Oligomeric Silsesquioxane Molecules. J. Polym. Sci. Part B: Polym. Phys. 2006, 44, 2122-2134.

[14] Joshi, M.; Butola, B. S. Isothermal Crystallization of HDPE/octamethyl Polyhedral Oligomeric Silsesquioxane Nanocomposites: Role of POSS as a Nanofiller. J. Appl. Polym. Sci. 2007, 105, 978-985.

[15] Hato, M. J.; Ray, S. S.; Luyt, A. S. Nanocomposites Based on Polyethylene and Polyhedral Oligomeric Silsesquioxanes, Microstructure, Thermal and Thermomechanical Properties. Macromol. Mater. Eng. 2008, 293, 752-762.